N.A.S.A. NGR-47-004-090
+
NGR-47-004-129

(NASA-CR-148813) A LIMITING ANALYSIS FOR EDGE EFFECTS IN ANGLE-PLY LAMINATES (Virginia Polytechnic Inst. and State Univ.) 34 p HC $4.00 CSCL 11D

N76-31301

Unclas
G3/24 03047

COLLEGE OF ENGINEERING

VIRGINIA POLYTECHNIC INSTITUTE AND STATE UNIVERSITY

BLACKSBURG, VIRGINIA

College of Engineering
Virginia Polytechnic Institute and State University
Blacksburg, Virginia 24061

VPI-E-76-18 September, 1976

A Limiting Analysis for Edge Effects in Angle-Ply Laminates

Peter W. Hsu
Carl T. Herakovich

Department of Engineering Science and Mechanics

Supported by NASA Grant NGR 47-004-090 and 47-004-129.

BIBLIOGRAPHIC DATA SHEET	1. Report No. VPI-E-76-18	2.	3. Recipient's Accession No.
4. Title and Subtitle A Limiting Analysis for Edge Effects in Angle-Ply Laminates			5. Report Date Sept., 1976 6.
7. Author(s) P. W. Hsu and Carl T. Herakovich			8. Performing Organization Rept. No. VPI-E-76-18
9. Performing Organization Name and Address Virginia Polytechnic Institute and State University Engineering Science and Mechanics Blacksburg, Virginia 24061			10. Project/Task/Work Unit No. 11. Contract/Grant No. NGR 47-004-090 NGR 47-004-129
12. Sponsoring Organization Name and Address National Aeronautics & Space Administration Langley Research Center Hampton, Virginia 23665			13. Type of Report & Period Covered 14.

15. Supplementary Notes

16. Abstracts

see page i

17. Key Words and Document Analysis. 17a. Descriptors

Composites, laminates, edge effects, interlaminar stresses, graphite/epoxy, perturbations

17b. Identifiers/Open-Ended Terms

17c. COSATI Field/Group

18. Availability Statement	19. Security Class (This Report) UNCLASSIFIED	21. No. of Pages 35
Distribution Unlimited	20. Security Class (This Page) UNCLASSIFIED	22. Price

INSTRUCTIONS FOR COMPLETING FORM NTIS-35 (Bibliographic Data Sheet based on COSATI Guidelines to Format Standards for Scientific and Technical Reports Prepared by or for the Federal Government, PB-180 600).

1. **Report Number.** Each individually bound report shall carry a unique alphanumeric designation selected by the performing organization or provided by the sponsoring organization. Use uppercase letters and Arabic numerals only. Examples FASEB-NS-73-87 and FAA-RD-73-09.

2. Leave blank.

3. **Recipient's Accession Number.** Reserved for use by each report recipient.

4. **Title and Subtitle.** Title should indicate clearly and briefly the subject coverage of the report, subordinate subtitle to the main title. When a report is prepared in more than one volume, repeat the primary title, add volume number and include subtitle for the specific volume.

5. **Report Date.** Each report shall carry a date indicating at least month and year. Indicate the basis on which it was selected (e.g., date of issue, date of approval, date of preparation, date published).

6. **Performing Organization Code.** Leave blank.

7. **Author(s).** Give name(s) in conventional order (e.g., John R. Doe, or J.Robert Doe). List author's affiliation if it differs from the performing organization.

8. **Performing Organization Report Number.** Insert if performing organization wishes to assign this number.

9. **Performing Organization Name and Mailing Address.** Give name, street, city, state, and zip code. List no more than two levels of an organizational hierarchy. Display the name of the organization exactly as it should appear in Government indexes such as Government Reports Index (GRI).

10. **Project/Task/Work Unit Number.** Use the project, task and work unit numbers under which the report was prepared.

11. **Contract/Grant Number.** Insert contract or grant number under which report was prepared.

12. **Sponsoring Agency Name and Mailing Address.** Include zip code. Cite main sponsors.

13. **Type of Report and Period Covered.** State interim, final, etc., and, if applicable, inclusive dates.

14. **Sponsoring Agency Code.** Leave blank.

15. **Supplementary Notes.** Enter information not included elsewhere but useful, such as: Prepared in cooperation with . . . Translation of . . . Presented at conference of . . . To be published in . . . Supersedes . . . Supplements . . . Cite availability of related parts, volumes, phases, etc. with report number.

16. **Abstract.** Include a brief (200 words or less) factual summary of the most significant information contained in the report. If the report contains a significant bibliography or literature survey, mention it here.

17. **Key Words and Document Analysis. (a). Descriptors.** Select from the Thesaurus of Engineering and Scientific Terms the proper authorized terms that identify the major concept of the research and are sufficiently specific and precise to be used as index entries for cataloging.
    (b). Identifiers and Open-Ended Terms. Use identifiers for project names, code names, equipment designators, etc. Use open-ended terms written in descriptor form for those subjects for which no descriptor exists.
    (c). COSATI Field/Group. Field and Group assignments are to be taken from the 1964 COSATI Subject Category List. Since the majority of documents are multidisciplinary in nature, the primary Field/Group assignment(s) will be the specific discipline, area of human endeavor, or type of physical object. The application(s) will be cross-referenced with secondary Field/Group assignments that will follow the primary posting(s).

18. **Distribution Statement.** Denote public releasability, for example "Release unlimited", or limitation for reasons other than security. Cite any availability to the public, other than NTIS, with address, order number and price, if known.

19 & 20. **Security Classification.** Do not submit classified reports to the National Technical Information Service.

21. **Number of Pages.** Insert the total number of pages, including introductory pages, but excluding distribution list, if any.

22. **NTIS Price.** Leave blank.

A LIMITING ANALYSIS FOR EDGE EFFECTS IN ANGLE-PLY LAMINATES[1]

Peter W. Hsu & Carl T. Herakovich
Department of Engineering Science & Mechanics
Virginia Polytechnic Institute & State University
Blacksburg, Virginia 24061

ABSTRACT

This paper develops a zeroth-order solution for edge effects in angle-ply composite laminates using perturbation techniques and a limiting free body approach. The general method of solution for $[\pm\theta]$ laminates is developed and then applied to the special case of a $[\pm 45]_s$ graphite/epoxy laminate. Interlaminar stress distributions are obtained as a function of the laminate thickness-to-width ratio h/b and compared to existing numerical results.

The solution predicts stable, continuous stress distributions, determines finite maximum tensile interlaminar normal stress σ_z for both $[\pm\theta]_s$ and $[\mp\theta]_s$ laminates, and provides mathematical evidence for singular interlaminar shear stresses τ_{xz} and τ_{yz} .

Introduction:

Recent numerical [1-6] and experimental [7-10] investigations have demonstrated the free edge effect in composite laminates subjected to remote tension. Such effect has been suggested to play the dominant role in the delamination failure initiation of some laminates. In an attempt to obtain more accurate free edge stress intensitites the problem of uniaxial extension of thin, elastic, balanced, symmetric, bidirectional laminates was investigated in an earlier paper [11] based upon a perturbation analysis [12,13]. A key feature of the analysis was the force and moment equilibrium of a limiting free body containing the interfacial plane between two layers. The interlaminar stresses thus obtained were compared with the finite difference solution of Pipes [6]. It was shown that the perturbation solution provides better results for the stress behavior near the free edge of the laminate.

The present paper presents a similar analysis for angle-ply laminates by perturbing the three coupled dimensionless partial differential equations resulting from a displacement formulation.

Governing Equations

For the balanced, symmetric 2m layer laminate of Fig. 1, the displacement functions take the following forms [2]:

$$\begin{aligned} u &= \xi_x x + \tilde{U}(y,z) && \text{(a)} \\ v &= \tilde{V}(y,z) && \text{(b)} \\ w &= \tilde{W}(y,z) && \text{(c)} \end{aligned} \qquad (1)$$

where ξ_x is the applied axial strain and $\tilde{U}(y,z)$, $\tilde{V}(y,z)$, and $\tilde{W}(y,z)$ are three unknown functions.

The dimensionless displacement equilibrium equations (with zero body forces) [14] are

$$\{Q_{66}(h/b)^2U_{,YY} + Q_{55}U_{,ZZ} + Q_{26}(h/b)^2V_{,YY} + Q_{45}V_{,ZZ} + (Q_{36} + Q_{45})(h/b)W_{,YZ}\}^{(k)} = 0$$

$$\{Q_{26}(h/b)^2U_{,YY} + Q_{45}U_{,ZZ} + Q_{22}(h/b)^2V_{,YY} + Q_{44}V_{,ZZ} + (Q_{23} + Q_{44})(h/b)W_{,YZ})\}^{(k)} = 0 \qquad (2)$$

$$\{(Q_{45} + Q_{36})(h/b)U_{,YZ} + (Q_{44} + Q_{23})(h/b)V_{,YZ} + Q_{44}(h/b)^2W_{,YY} + Q_{33}W_{,ZZ}\}^{(k)} = 0$$

where $Q_{ij}^{(k)} = C_{ij}^{(k)}/C_{max}^{(k)}$ with $C_{ij}^{(k)}$ being the transformed stiffness coefficients of the material properties from the natural coordinates to the xy coordinates, and $C_{max}^{(k)}$ the largest stiffness coefficient of the k^{th} layer. $Y = y/b$, $Z = z/h$ are the dimensionless coordinates, and $U = \tilde{U}/h$, $V = \tilde{V}/h$, and $W = \tilde{W}/h$ are the dimensionless unknown displacement functions. Symmetry conditions lead to [14]

$$\begin{aligned} U(Y,Z) &= U(Y,-Z) && \text{(a)}\\ V(Y,Z) &= V(Y,-Z) && \text{(b)}\\ W(Y,Z) &= -W(Y,-Z) && \text{(c)}\\ U(Y,Z) &= -U(-Y,Z) && \text{(d)}\\ V(Y,Z) &= -V(-Y,Z) && \text{(e)}\\ W(Y,Z) &= W(-Y,Z) && \text{(f)} \end{aligned} \qquad (3)$$

which yield the following symmetry constraints on the displacement functions:

$$\begin{aligned} \{U_{,z}(y,0)\}^{(m)} &= 0\\ \{V_{,z}(y,0)\}^{(m)} &= 0\\ \{W(y,0)\}^{(m)} &= 0 \end{aligned} \qquad (4)$$

$$\begin{aligned} \{U(0,z)\}^{(k)} &= 0\\ \{V(0,z)\}^{(k)} &= 0\\ \{W_{,y}(0,z)\}^{(k)} &= 0 \end{aligned} \qquad (5)$$

where m denotes the layer adjacent to the midplane Z = 0, and arbitrary layers are denoted by k.

The appropriate stress free boundary conditions can be expressed as:

$$\sigma_y^{(k)}(\pm1,Z) = \{\frac{C_{12}\varepsilon_x}{h} + \frac{C_{22}}{b} V_{,Y}(\pm1,Z) + \frac{C_{23}}{h} W_{,Z}(\pm1,Z) + \frac{C_{26}}{b} U_{,Y}(\pm1,Z)\}^{(k)}=0 \qquad \text{(a)}$$

$$\tau_{xy}^{(k)}(\pm1,Z) = \{\frac{C_{16}\varepsilon_x}{h} + \frac{C_{26}}{b} V_{,Y}(\pm1,Z) + \frac{C_{36}}{h} W_{,Z}(\pm1,Z) + \frac{C_{66}}{b} U_{,Y}(\pm1,Z)\}^{(k)}=0 \qquad \text{(b)(6)}$$

$$\tau_{yz}^{(k)}(\pm1,Z) = \{\frac{C_{44}}{h} V_{,Z}(\pm1,Z) + \frac{C_{44}}{b} W_{,Y}(\pm1,Z) + \frac{C_{45}}{h} U_{,Z}(\pm1,Z)\}^{(k)}=0 \qquad \text{(c)}$$

along the free edges, and

$$\sigma_z^{(1)}(Y,\pm1) = \{\frac{C_{13}\varepsilon_x}{h} + \frac{C_{23}}{b} V_{,Y}(Y,\pm1) + \frac{C_{33}}{h} W_{,Z}(Y,\pm1) + \frac{C_{36}}{b} U_{,Y}(y,\pm1)\}^{(1)}= 0 \qquad \text{(a)}$$

$$\tau_{yz}^{(1)}(Y,\pm1) = \{\frac{C_{44}}{h} V_{,Z}(Y,\pm1) + \frac{C_{44}}{b} W_{,Y}(Y,\pm1) + \frac{C_{45}}{h} U_{,Z}(Y,\pm1)\}^{(1)}= 0 \qquad \text{(b)(7)}$$

$$\tau_{xz}^{(1)}(Y,\pm1) = \{\frac{C_{45}}{h} V_{,Z}(Y,\pm1) + \frac{C_{45}}{b} W_{,Y}(Y,\pm1) + \frac{C_{55}}{h} U_{,Z}(Y,\pm1)\}^{(1)}= 0 \qquad \text{(c)}$$

on the top and the bottom surfaces.

To solve the boundary value problem defined by Equations (2) and (4)-(7), only the first quadrant of the YZ-plane needs to be considered due to the favorable symmetry of the laminate. Recognizing that the boundary layer effect exists near the free edge Y = 1, the perturbation solution is sought by considering two regions of the laminate: the interior region (away from the free edge) and the boundary layer region (near the free edge).

Perturbation Solution

(1) The interior region ($0 \leq Y < 1$)

In this region the free edge stress boundary conditions (6) are dropped and attention is focused on the solution to Equations (2) subject to Equations (4), (5) and (7). To seek a straight forward asymptotic expansion, let

$$U^{(k)} = \sum_{n=0}^{\infty} \varepsilon^n U_n^{(k)}(Y,Z)$$

$$V^{(k)} = \sum_{n=0}^{\infty} \varepsilon^n V_n^{(k)}(Y,Z) \tag{8}$$

$$W^{(k)} = \sum_{n=0}^{\infty} \varepsilon^n W_n^{(k)}(Y,Z) \qquad k = 1,2,3,\ldots,m$$

where the subscript i denotes the interior region and the small parameter $\varepsilon(<<1)$ represents the thickness-to-width ratio h/b. Substituting these expansions into Equations (2) and equating coefficients of equal powers of ε to zero result in infinite sets of equations. The zeroth-order equations take the form

$$\begin{aligned} \varepsilon^0 : \left\{Q_{55}U_{o,ZZ} + Q_{45}V_{o,ZZ}\right\}^{(k)} &= 0 \\ \left\{Q_{45}U_{o,ZZ} + Q_{44}V_{o,ZZ}\right\}^{(k)} &= 0 \\ \left\{Q_{33}W_{o,ZZ}\right\}^{(k)} &= 0 \end{aligned} \tag{9}$$

As a result of the symmetry conditions (3), Equations (9) have solution in the form

$$\begin{aligned} U_o^{(k)} &= B_o^{(k)}(Y) \\ V_o^{(k)} &= D_o^{(k)}(Y) \\ W_o^{(k)} &= E_o^{(k)}Z \end{aligned} \tag{10}$$

where $B_o^{(k)}(Y)$, $D_o^{(k)}(Y)$, $E_o^{(k)}$ must satisfy the vanishing stress conditions to recover the lamination theory in this interior region. That is,

$$\{C_{13}\varepsilon_x(1-\varepsilon)Y/h + \frac{C_{23}}{b} D_o(Y) + \frac{C_{33}}{h} E_oY + \frac{C_{36}}{b} B_o(Y)\}^{(k)} = 0 \tag{11}$$

which are in effect generalizations of Equations (7a) which satisfy the symmetry constraints (4) and (5). The nonzero central plane stresses are now required to satisfy the equilibrium conditions (Fig. 2):

$$\sum_{k=1}^{m}\left(\sigma_y^{(k)}(0,Z)h_k\right) = h\left\{\sum_{k=1}^{m}\left(C_{12}(1-\epsilon)/h + \frac{C_{23}}{h}E_0\right)^{(k)} h_k \epsilon_x + \sum_{k=1}^{m}\frac{C_{22}^{(k)}h_k}{b} D_0^{(k)\prime}(Y) + \sum_{k=1}^{m}\frac{C_{26}^{(k)}h_k}{b} B_0^{(k)\prime}(Y)\right\} = 0 \qquad (12)$$

$$\sum_{k=1}^{m}\left(\tau_{xy}^{(k)}(0,Z)h_k\right) = h\left\{\sum_{k=1}^{m}\left(C_{16}(1-\epsilon)/h + \frac{C_{36}}{h}E_0\right)^{(k)} h_k \epsilon_x + \sum_{k=1}^{m}\frac{C_{26}^{(k)}h_k}{b} D_0^{(k)\prime}(Y) + \sum_{k=1}^{m}\frac{C_{66}^{(k)}h_k}{b} B_0^{(k)\prime}(Y)\right\} = 0 \qquad (13)$$

Enforcing exact displacement continuities in U and V across each interface, yields

$$B_0^{(1)}(Y) = B_0^{(2)}(Y) = \dots = B_0^{(k)}(Y) = \bar{B}_0(Y) \qquad (14)$$

$$D_0^{(1)}(Y) = D_0^{(2)}(Y) = \dots = D_0^{(k)}(Y) = \bar{D}_0(Y) \qquad (15)$$

These equations reduce Equations (11)-(13) to m+2 equations for the m+2 unknowns $\bar{B}_0(Y)$, $\bar{D}_0(Y)$, $E_0^{(k)}$. The solution to these reduced equations uniquely determines the zeroth-order interior region solution (10). This is the solution from lamination theory as will be demonstrated later for a four layer angle-ply laminate.

It is important to note that although exact displacement continuity in W was not imposed in the interior region, it will be shown to be satisfied automatically for angle-ply laminates.

(2) The boundary layer region ($Y=1$)

Introducing the stretching transformation

$$\eta = (1-Y)/(\frac{h}{b}) \tag{16}$$

near the free edge $Y = 1$ to the governing equations (2) results in the following equations:

$$\begin{aligned}
&\{Q_{66}U_{,\eta\eta} + Q_{55}U_{,ZZ} + Q_{26}V_{,\eta\eta} + Q_{45}V_{,ZZ} - (Q_{36} + Q_{45})W_{,\eta Z}\}^{(k)} = 0 \quad (a)\\
&\{Q_{26}U_{,\eta\eta} + Q_{45}U_{,ZZ} + Q_{22}V_{,\eta\eta} + Q_{44}V_{,ZZ} - (Q_{23} + Q_{44})W_{,\eta Z}\}^{(k)} = 0 \quad (b)\\
&\{-(Q_{45} + Q_{36})U_{,\eta Z} - (Q_{44} + Q_{23})V_{,\eta Z} + Q_{44}W_{,\eta\eta} + Q_{33}W_{,ZZ}\}^{(k)} = 0 \quad (c)
\end{aligned} \tag{17}$$

To seek a solution which satisfies the symmetry conditions (3), the constraint equations (4), and the asymptotic recovery of the lamination theory for large η, the following expansions are assumed:

$$\begin{aligned}
U_b^{(k)} &= \sum_{n=0}^{\infty} [B_n(Y) + P_n e^{\lambda_n \eta} \cos \alpha_n Z]^{(k)} \varepsilon^n\\
V_b^{(k)} &= \sum_{n=0}^{\infty} [D_n(Y) + R_n e^{\lambda_n \eta} \cos \alpha_n Z]^{(k)} \varepsilon^n\\
W_b^{(k)} &= \sum_{n=0}^{\infty} [E_n Z + S_n e^{\lambda_n \eta} \sin \alpha_n Z]^{(k)} \varepsilon^n
\end{aligned} \tag{18}$$

where $B_n^{(k)}$, $D_n^{(k)}$, $E_n^{(k)}$ are the interior region solution given by Equations (11)-(15), $P_n^{(k)}$, $R_n^{(k)}$ and $S_n^{(k)}$ are undetermined coefficients, and $\alpha_n^{(k)}$ are undetermined positive quantities (in radians). The subscript b denotes the boundary layer region.

Substituting Equations (18) into Equations (17) and neglecting higher-order terms results in the following set of three simultaneous algebraic equations corresponding to the order ε^0:

$$\{(Q_{66}\lambda_o^2 - Q_{55}\alpha_o^2)P_o + (Q_{26}\lambda_o^2 - Q_{45}\alpha_o^2)R_o - (Q_{36} + Q_{45})\lambda_o\alpha_o S_o\}^{(k)} = 0$$
$$\{(Q_{26}\lambda_o^2 - Q_{45}\alpha_o^2)P_o + (Q_{22}\lambda_o^2 - Q_{44}\alpha_o^2)R_o - (Q_{23} + Q_{44})\lambda_o\alpha_o S_o\}^{(k)} = 0 \quad (19)$$
$$\{(Q_{45} + Q_{36})\lambda_o\alpha_o P_o + (Q_{44} + Q_{23})\lambda_o\alpha_o R_o + (Q_{44}\lambda_o^2 - Q_{33}\alpha_o^2)S_o\}^{(k)} = 0$$
$$k = 1,2,\ldots,m$$

For each nontrivial term of Equations (18) to exist the determinants of the algebraic equations (19) must vanish individually. This leads to a sixth-order algebraic equation for each layer which can be regarded as a third-order equation by classical treatment [15]. The six roots may be expressed as

$$\begin{aligned} &\{\lambda_o(1,2) = \pm\, \bar{a}\ \alpha_o\}^{(k)} \\ &\{\lambda_o(3,4) = \pm\, \bar{b}\ \alpha_o\}^{(k)} \qquad (20) \\ &\{\lambda_o(5,6) = \pm\, \bar{c}\ \alpha_o\}^{(k)} \end{aligned}$$

where $\bar{a}^{(k)}$, $\bar{b}^{(k)}$, $\bar{c}^{(k)}$ are three constants in terms of the material properties of the k^{th} layer. For matching considerations, however, the positive roots must be dropped since they lead to exponential growth of the displacement, strain and stress fields for large η (or small Y). Hence, the zeroth-order expansions of Equations (18) take the following general form:

$$U_b^{(k)} = \{B_o(Y) + (P_1 e^{-\bar{a}\alpha_o\eta} + P_2 e^{-\bar{b}\alpha_o\eta} + P_3 e^{-\bar{c}\alpha_o\eta}) \cos \alpha_o Z\}^{(k)}$$
$$V_b^{(k)} = \{D_o(Y) + (R_1 e^{-\bar{a}\alpha_o\eta} + R_2 e^{-\bar{b}\alpha_o\eta} + R_3 e^{-\bar{c}\alpha_o\eta}) \cos \alpha_o Z\}^{(k)} \quad (21)$$
$$W_b^{(k)} = \{E_o Z + (S_1 e^{-\bar{a}\alpha_o\eta} + S_2 e^{-\bar{b}\alpha_o\eta} + S_3 e^{-\bar{c}\alpha_o\eta}) \sin \alpha_o Z\}^{(k)}$$

where P_o has been replaced by P_1, P_2, P_3, etc.

It may be shown that due to the separate variable nature of Equations (21), no exact satisfaction of the free edge stress boundary conditions (6a) and (6b) (for all Z) and the stress boundary conditions (7) on the top and bottom surfaces (for all Y) can be achieved. By arguing that higher-order terms serve as correction terms, attention can now be focused on points (η=0,Z_k+ζ) and (η=0,Z_k-ζ) on the free edge (Fig. 3). That is, requiring exact satisfaction of the boundary conditions (6a,6b,6c) at these points only [11,14] with Equations (21) and considering the resulting force and moment equilibrium of the limiting free body of thickness 2ζ (0<ζ<<<1) result in the algebraic equations:

$$\begin{aligned}
&\{[C_{26}(\bar{a}P_1+\bar{b}P_2+\bar{c}P_3) + C_{22}(\bar{a}R_1+\bar{b}R_2+\bar{c}R_3)\\
&\quad + C_{23}(S_1+S_2+S_3)]\alpha_o\cos(\alpha_o(Z_k\pm\zeta)) \qquad \text{(a)}\\
&= -[\, C_{12}\frac{(1-\varepsilon)\varepsilon}{h}{}_x + \frac{C_{23}}{h}E_o + \frac{C_{22}}{b}D_o'(\pm 1) + \frac{C_{26}}{b}B_o(\pm 1)]h\}^{(k)}
\end{aligned}$$

$$\begin{aligned}
&\{[C_{66}(\bar{a}P_1+\bar{b}P_2+\bar{c}P_3) + C_{26}(\bar{a}R_1+\bar{b}R_2+\bar{c}R_3)\\
&\quad + C_{36}(S_1+S_2+S_3)]\alpha_o\cos(\alpha_o(Z_k\pm\zeta)) \qquad \text{(b)(22)}\\
&= -[\, C_{16}\frac{(1-\varepsilon)\varepsilon}{h}{}_x + \frac{C_{36}}{h}E_o + \frac{C_{26}}{b}D_o'(\pm 1) + \frac{C_{66}}{b}B_o(\pm 1)]h\}^{(k)}
\end{aligned}$$

$$\{C_{44}[(R_1+R_2+R_3) - (S_1\bar{a}+S_2\bar{b}+S_3\bar{c})] + C_{45}(P_1+P_2+P_3)\}^{(k)} = 0 \qquad \text{(c)}$$

$$k = 1,2,\ldots\ldots,m$$

Note that the right hand sides of Equations (22a) and (22b) are all known quantities from the interior region solution. Solving nine equations (three from (17a), three from (17b) and three boundary conditions (22a)-(22c)) leads to the determination of the nine unknown coefficients P_i, R_i, S_i (i=1,3) in terms of $\alpha_o^{(k)}$. The validity of the solution thus obtained can be readily checked by the self-equilibrating condition of the stress resultant

$$\int_0^b \sigma_z^{(k)} dY = 0 \tag{23}$$

for any level of Z. Finally, equating the force and moment resulting from the boundary layer displacement fields (21) with the interior region stress resultants determines the values of $\alpha_o^{(k)}((Z_k \pm \zeta))$ to their order of accuracy. Thus, the "near-interlaminar" stress distributions can be obtained based upon a reference layer. It should be noted that displacement continuity in this boundary layer region has not yet been imposed as a physical requirement. It will be imposed subsequently in a numerical example.

Four Layer Angle-Ply Laminates

For advanced fiber-reinforced composites having three mutually perpendicular planes of elastic symmetry, the stiffness coefficients $C_{45}^{(k)}$ vanish. For a four layer angle-ply laminate with symmetric [±θ] orientations (Fig. 4a), the following relations between material constants (with respect to xyz coordinates) are found to exist [14]

$$C_{ij}^{(1)} = C_{ij}^{(2)} \quad , \quad i = 1,2,3 \text{ and } j = 1,2,3$$

$$C_{kk}^{(1)} = C_{kk}^{(2)} \quad , \quad k = 4,5,6$$

$$C_{n6}^{(1)} = - C_{n6}^{(2)} \quad , \quad n = 1,2,3$$

The zeroth-order interior region solution (10) yields

$$
\begin{aligned}
U_o^{(1)} &= U_o^{(2)} = 0 \\
V_o^{(1)} &= V_o^{(2)} = -\frac{(C_{12}C_{33} - C_{13}C_{23})^{(1)}\varepsilon_x bY(1-\varepsilon)}{(C_{22}C_{33} - C_{23}C_{23})^{(1)}h} \\
W_o^{(1)} &= W_o^{(2)} = -\frac{(C_{13}C_{22} - C_{12}C_{23})^{(1)}\varepsilon_x Z(1-\varepsilon)}{(C_{22}C_{33} - C_{23}C_{23})^{(1)}}
\end{aligned}
\tag{24}
$$

It can be seen from (24) that the exact continuity in W results automatically.

On the central plane (Y=0), the stresses are obtained by combining Equations (24), the constitutive equations, and the strain-displacement relations. The results are

$$\sigma_y^{(1)}(0,Z) = \sigma_y^{(2)}(0,Z) = 0 \tag{a}$$

$$
\begin{aligned}
\tau_{xy}^{(1)}(0,Z) &= -\tau_{xy}^{(2)}(0,Z) \\
&= \left[C_{16} - \frac{C_{26}(C_{12}C_{33} - C_{13}C_{23}) + C_{36}(C_{13}C_{22} - C_{12}C_{33})}{(C_{22}C_{33} - C_{23}C_{23})}\right]^{(1)} \varepsilon_x(1-\varepsilon) \quad \text{(b)}
\end{aligned}
\tag{25}
$$

which indicates that the lamination theory (or the zeroth-order interior region solution) contributes no normal stress along the central plane Y=0. For equilibrium considerations the interlaminar shear stress resultant and the couple moment due to the interlaminar normal stress σ_z should both be expected to vanish (Fig. 5). Thus, two more self-equilibrating conditions are established, in addition to Equation (23), as

$$\int_0^b \tau_{yz}\, dy = 0 \tag{26}$$

$$\int_0^b \sigma_z\, y dy = 0 \tag{27}$$

where τ_{yz} and σ_z are both determined by solving the boundary layer equations (16-22) with k=1,2.

Numerical example

(1) $[45/-45]_s$ graphite-epoxy laminate

Consider the $[45/-45]_s$ graphite-epoxy laminate of constant layer thickness h/2 (Fig. 4a). The material properties are

$$\begin{aligned} E_{11} &= 20 \times 10^6 \text{ (psi)} \\ E_{22} = E_{33} &= 2.1 \times 10^6 \text{(psi)} \\ G_{12} = G_{23} = G_{13} &= 0.85 \times 10^6 \text{(psi)} \\ \nu_{12} = \nu_{23} = \nu_{13} &= 0.21 \end{aligned} \tag{28}$$

The transformed stiffness coefficients are

$$\begin{array}{ll} \underline{45(\times 10^{-6}\text{ psi})} & \underline{-45(\times 10^{-6}\text{ psi})} \\ C_{11}^{(1)} = 6.745 & C_{11}^{(2)} = 6.745 \\ C_{12}^{(1)} = 5.045 & C_{12}^{(2)} = 5.045 \\ C_{13}^{(1)} = 0.521 & C_{13}^{(2)} = 0.521 \\ C_{22}^{(1)} = 6.745 & C_{22}^{(2)} = 6.745 \\ C_{23}^{(1)} = 0.521 & C_{23}^{(2)} = 0.521 \\ C_{33}^{(1)} = 2.213 & C_{33}^{(2)} = 2.213 \\ C_{16}^{(1)} = C_{26}^{(1)} = -4.506 & C_{16}^{(2)} = C_{26}^{(2)} = 4.506 \\ C_{36}^{(1)} = -0.04387 & C_{36}^{(2)} = 0.04387 \\ C_{44}^{(1)} = C_{55}^{(1)} = 0.85 & C_{44}^{(2)} = C_{55}^{(2)} = 0.85 \\ C_{66}^{(1)} = 5.33 & C_{66}^{(2)} = 5.33 \\ C_{45}^{(1)} = 0 & C_{45}^{(2)} = 0 \end{array} \tag{29}$$

The interior solution (24) yields

$$
\begin{aligned}
U_o^{(1)} &= U_o^{(2)} = 0 \\
V_o^{(1)} &= V_o^{(2)} = -0.7433\ \xi_x \frac{b}{h} Y(1-\varepsilon) \\
W_o^{(1)} &= W_o^{(2)} = -0.0604\ \xi_x Z\ (1-\varepsilon)
\end{aligned}
\tag{30}
$$

which lead to the central plane stresses

$$
\begin{aligned}
\tau_{xy}^{(1)}(0,Z) &= -\ \tau_{xy}^{(2)}(0,Z) = 1.154\ \xi_x(1-\varepsilon)(10^6\text{psi}) \\
\sigma_y^{(1)}(0,Z) &= -\ \sigma_y^{(2)}(0,Z) = 0
\end{aligned}
\tag{31}
$$

The boundary layer equation (17-19) yield two identical sixth-order algebraic equations [14] which give three pairs of real roots. For matching considerations only the three negative roots are taken. Finally the composite solution (in the perturbation sense) is formed as

$$
\begin{aligned}
U_c^{(k)} &= \{(P_1 e^{-\beta_1\alpha_o\eta} + P_2 e^{-\beta_2\alpha_o\eta} + P_3 e^{-\beta_3\alpha_o\eta})\cos \alpha_o Z\}^{(k)} \\
V_c^{(k)} &= -\ 0.7433\ \xi_x(1-\varepsilon)\frac{b}{h}\ Y + \{(R_1 e^{-\beta_1\alpha_o\eta} + R_2 e^{-\beta_2\alpha_o\eta} \\
&\qquad + R_3 e^{-\beta_3\alpha_o\eta})\cos \alpha_o Z\}^{(k)} \\
W_c^{(k)} &= -\ 0.0604\ \xi_x(1-\varepsilon)Z + \{(S_1 e^{-\beta_1\alpha_o\eta} + S_2 e^{-\beta_2\alpha_o\eta} \\
&\qquad + S_3 e^{-\beta_3\alpha_o\eta})\sin \alpha_o Z\}^{(k)}
\end{aligned}
\tag{32}
$$

where

$$
\begin{aligned}
\beta_1^{(k)} &= 1.2364 \\
\beta_2^{(k)} &= 0.2903 \\
\beta_3^{(k)} &= 0.9659
\end{aligned}
$$

Exact satisfaction of the governing equations and the boundary conditions at points (η=0,1/2+ζ) and (η=0,1/2-ζ) leads to the following equations:

$$
\begin{aligned}
P_1^{(1)} &= -\,0.5871\ \phi_1 \quad, & P_1^{(2)} &= 0.5871\ \phi_2 \\
P_2^{(1)} &= 0.1707\ \phi_1 \quad, & P_2^{(2)} &= -\,0.1707\ \phi_2 \\
P_3^{(1)} &= 1.2021\ \phi_1 \quad, & P_3^{(2)} &= -\,1.2021\ \phi_2 \\
R_1^{(1)} &= -\,0.6309\ \phi_1 \quad, & R_1^{(2)} &= -\,0.6309\ \phi_2 \\
R_2^{(1)} &= -\,0.1813\ \phi_1 \quad, & R_2^{(2)} &= -\,0.1813\ \phi_2 \\
R_3^{(1)} &= 1.1897\ \phi_1 \quad, & R_3^{(2)} &= 1.1897\ \phi_2 \\
S_1^{(1)} &= 1.1358\ \phi_1 \quad, & S_1^{(2)} &= 1.1358\ \phi_2 \\
S_2^{(1)} &= 0.0347\ \phi_1 \quad, & S_2^{(2)} &= 0.0347\ \phi_2 \\
S_3^{(1)} &= -\,1.0736\ \phi_1 \quad, & S_3^{(2)} &= -\,1.0736\ \phi_2
\end{aligned}
\tag{33}
$$

where

$$
\begin{aligned}
\phi_1 &= \frac{\xi_x\,(1-\varepsilon)}{\alpha_o^{(1)}\cos\left(\alpha_o^{(1)}\left(\frac{1}{2}+\zeta\right)\right)} \\
\phi_2 &= \frac{\xi_x\,(1-\varepsilon)}{\alpha_o^{(2)}\cos\left(\alpha_o^{(2)}\left(\frac{1}{2}-\zeta\right)\right)} \\
& \qquad\qquad 0 < \zeta \lll 1
\end{aligned}
\tag{34}
$$

It can be shown that these coefficients lead to identical satisfaction of the self-equilibrating conditions (Equations (23) and (26)) when the lower limit is replaced by infinity - the corresponding zeroth-order domain of the interior region. Furthermore, requiring the force equilibrium condition

$$\int_0^b \tau_{xz}^{(k)}\ (y,\ 1/2 \pm \zeta)\ dy + \tau_{xy}^{(k)}\ (0,z)\ \frac{h}{2} = 0$$

leads to

$$\frac{\tan\left(\frac{\alpha_o^{(k)}}{2} \pm \zeta\ \alpha_o^{(k)}\right)}{\alpha_o^{(k)}} = 0.5 \qquad (0 < \zeta <<< 1) \tag{35}$$

Now consider Equations (32) and (33). It is clear that Layer 1 (+45^o) and Layer 2 (-45^o) are antisymmetric in U and symmetric in both V and W with respect to the infinitesimal thin slice (Fig. 4d). Upon enforcing exact continuity in displacement U, V, W at Z = 1/2, the following equation is obtained

$$\lim_{\zeta\to 0} \cos\left[\frac{\alpha_o^{(1)}}{2} + \alpha_o^{(1)}\zeta\right] = \lim_{\zeta\to 0} \cos\left[\frac{\alpha_o^{(2)}}{2} - \alpha_o^{(2)}\zeta\right] = 0 \tag{36}$$

which yields

$$\cos\left[\frac{\alpha_o^{(1)}}{2} + \zeta\ \alpha_o^{(1)}\right] = \cos\left[\frac{\alpha_o^{(2)}}{2} - \zeta\ \alpha_o^{(2)}\right] \doteq 0 \tag{37}$$

$$\text{for } 0 < \zeta <<< 1$$

and

$$\lim_{\zeta\to 0}\left|\tan\left[\frac{\alpha_o^{(k)}}{2} \pm \alpha_o^{(k)}\zeta\right]\right| = \infty \tag{38}$$

The interlaminar stresses based upon the lower layer (-45°) may now be expressed from the stress-displacement relations as

$$\tau_{xz} = (0.85 \times 10^{6})(1-\varepsilon)\xi_{x}[-0.5871e^{-1.2364\alpha\eta} + 0.1707e^{-0.2903\alpha\eta} + 1.2021e^{-0.9659\alpha\eta}]\tan(\tfrac{\alpha}{2} - \alpha\zeta) \qquad \text{(a)}$$

$$\tau_{yz} = (0.85 \times 10^{6})(1-\varepsilon)\xi_{x}[2.0350e^{-1.2364\alpha\eta} + 0.1913e^{-0.2903\alpha\eta} - 2.2263e^{-0.9659\alpha\eta}]\tan(\tfrac{\alpha}{2} - \alpha\zeta) \qquad \text{(b)} \qquad (39)$$

$$\sigma_{z} = (1-\varepsilon)\xi_{x}(10^{6})[2.1389e^{-1.2364\alpha\eta} + 0.0472e^{-0.2903\alpha\eta} - 1.8281e^{-0.9659\alpha\eta}] \qquad \text{(c)}$$

$$0<\zeta<<<1$$

If the stacking sequence is reversed to $[-45/45]_{s}$, (Fig. 4e) the interlaminar stresses become

$$\tau_{xz} = (0.85 \times 10^{6})(1-\varepsilon)\xi_{x}[+0.5871e^{-1.2364\alpha\eta} - 0.1707e^{-0.2903\alpha\eta} - 1.2021e^{-0.9659\alpha\eta}]\tan(\tfrac{\alpha}{2} - \alpha\zeta) \qquad \text{(a)}$$

$$\tau_{yz} = (0.85 \times 10^{6})(1-\varepsilon)\xi_{x}[2.0350e^{-1.2364\alpha\eta} + 0.1913e^{-0.2903\alpha\eta} - 2.2263e^{-0.9659\alpha\eta}]\tan(\tfrac{\alpha}{2} - \alpha\zeta) \qquad \text{(b)} \qquad (40)$$

$$\sigma_{z} = (1-\varepsilon)\xi_{x}(10^{6})[2.1389e^{-1.2364\alpha\eta} + 0.0472e^{-0.2903\alpha\eta} - 1.8281e^{-0.9659\alpha\eta}] \qquad \text{(c)}$$

$$0<\zeta<<<1$$

Results and Discussion

From Equations (39) and (40) it is clear that the interlaminar shear stresses τ_{xz} and τ_{yz} are both proportional to the near singular value of

$\tan(\frac{\alpha}{2} - \alpha\zeta)$ which results from Equation (35 & 38). Hence α serves as a problem parameter which may be more realistically determined experimentally. Figure 6 shows the influence of α on the interlaminar shear stress τ_{xz}. Obviously, τ_{xz} becomes more singular as α is increased and may attain a much higher finite maximum value at the free edge than the calculated finite difference result of [3]*. This is in agreement with the work of Pipes and Pagano [7] in which they found that τ_{xz} tends to grow without bound. Figure 7 shows the interlaminar shear stress τ_{yz} as a function of the problem parameter α. Although τ_{yz} is proportional to the near singular value $\tan(\frac{\alpha}{2} -\alpha\zeta)$ $(0<\zeta<<<1)$ it is zero at the free edge thus satisfying the stress free boundary condition. It should be noted that τ_{yz} attains larger peak values, for higher values of α. The negative-positive variation of τ_{yz} confirms the validity of the self-equilibrating condition (26). The finite difference solution, however, does not predict such variation. In a later paper, it will be shown that the negative-positive variation agrees well with the finite element result by Renieri [16] which further supports the present theory. The variation of the interlaminar normal stress σ_z in Fig. 8 (Eqn. 40c) indicates that the maximum finite value of σ_z at the free edge is independent of the problem parameter α. The only influence of α on σ_z lies in the boundary layer width. The positive-negative (tensile-compressive) variation of σ_z confirms the solution validity by satisfying the self-equilibrating condition (23). The finite difference results, on the other hand, indicate instability near the free edge [14].

The present theory (Eqns. (8) - (22)) is based upon the zeroth-order analysis of the geometric ratio h/b. Hence the smaller h/b, the better the

---

* All finite difference reuslts presented in this paper were obtained by the authors using the program supplied by Professor Pipes.

solution accuracy [14]. The effects of this ratio on the interlaminar stress components can be observed in Figs. 9-11. In Fig. 9, for a smaller h/b, τ_{xz} has a smaller boundary layer width while attaining a higher maximum value at the free edge (for a fixed α). Similar behavior is found for τ_{yz} (Fig. 10) where the stress attains a higher peak value and a smaller boundary layer width for a smaller h/b. In Fig. 11, a higher $\sigma_{z\ max}$ and a smaller boundary layer width are obtained for a smaller h/b. The interlaminar stress distributions for the reversed stacking sequence $[-45/45]_s$ Gr/E are not plotted. However it is important to point out [14] that only τ_{xz} experiences a sign reversal when the stacking sequence is reversed. The sign of the remaining two components of interlaminar stress is not a function of the stacking sequence. Thus for reliable design fo angle-ply laminates, the delamination failure mode due to the tensile σ_z at the free edge should always be taken into consideration.

Conclusions

A method of solution for the problem of elastic, balanced, symmetric laminates subject to uniaxial extension has been developed based upon the perturbation theory. Attention has been focused on the force and moment equilibrium for an infinitesimally thin slice containing the interfacial plane. The solution provides better insight into the free edge interlaminar stress behavior for thin angle-ply laminates (h/b<<1) than existing numerical solutions.

Acknowledgements

This investigation was supported by NASA Grants NGR 47-004-090 and NGR 47-004-129. Dr. John G. Davis of the Composites Section, NASA Langley Research Center was the technical monitor. The authors are also indebted to Professor R. Byron Pipes of the University of Delaware for supplying his finite difference program, to Professor Ali H. Nayfeh of VPI & SU for his helpful assistance with the perturbation technique and to Mrs. Frances Carter for typing the manuscript.

REFERENCES

1. A. H. Puppo and H. A. Evensen, "Interlaminar Shear in Laminated Composites Under Plane Stress," J. Composite Materials, Vol. 4 (1970) p. 204.

2. R. B. Pipes and N. J. Pagano, "Interlaminar Stresses in Composite Laminates Under Uniform Axial Extension," J. Composite Materials, Vol. 4 (1970), p. 538.

3. G. Isakson and A. Levy, "Finite-Element Analysis of Interlaminar Shear in Fibrous Composites," J. Composite Materials, Vol. 5 (1971), p. 273.

4. A. Levy, H. Armen, Jr., and J. Whiteside, "Elastic and Plastic Interlaminar Shear Deformation in Laminated Composites Under Generalized Plane Stress," Proc. of 3rd Conference on Matrix Methods in Structural Mechanics, Wright Patterson Air Force Base, Ohio, (1969).

5. E. F. Rybicki, "Approximate Three-Dimensional Solutions for Symmetric Laminates Under Inplane Loading," J. Composite Materials, Vol. 5 (1971), p. 354.

6. R. B. Pipes, "Interlaminar Stresses in Composite Laminates," AFML-TR-72-18, 1972.

7. R. B. Pipes and I. M. Daniel, "Moire' Analysis of the Interlaminar Shear Edge Effect in Laminated Composites," J. Composite Materials, Vol. 5, (1971), p. 255.

8. C. T. Herakovich, "Tensile Strength Behavior of Composite Reinforced Metals," VPI-E-72-11, (1972), p. 54.

9. D. W. Oplinger, B. S. Parker, and F. P. Chiang, "Edge Effect Studies in Fiber-Reinforced Laminates,' AMMRC-TR-73-41, Army Materials and Mechanics Research Center, Watertown, Massachusetts.

10. N. J. Pagano and R. B. Pipes, "Some Observations on the Interlaminar Strength of Composite Laminates," Int. J. Mech. Sci., Vol. 15 (1973), pp. 679-688.

11. P. W. Hsu and C. T. Herakovich, "A Perturbation Solution for Interlaminar Stresses in Composite Laminates," ASTM 4th Conference on Composite Materials: Testing and Design, Valley Forge, Pa., May, 1976.

12. A. H. Nayfeh, Perturbation Methods, Wiley-Interscience, New York, (1973).

13. M. Van Dyke, Perturbation Methods in Fluid Mechanics, Academic Press, New York and London, (1964).

14. P. W. Hsu, "Interlaminar Stresses in Composite Laminates - A Perturbation Analysis," Ph.D. Dissertation, VPI & SU, Blacksburg, Va., Jan. 1976.

15. J. W. Archbold, Algebra, Sir Isaac Pitman and Sons, London, (1964), p. 174.

16. G. D. Renieri, "Nonlinear Analysis of Laminated Fibrous Composite," Ph.D. Dissertation, VPI & SU, Blacksburg, Va., June, 1976.

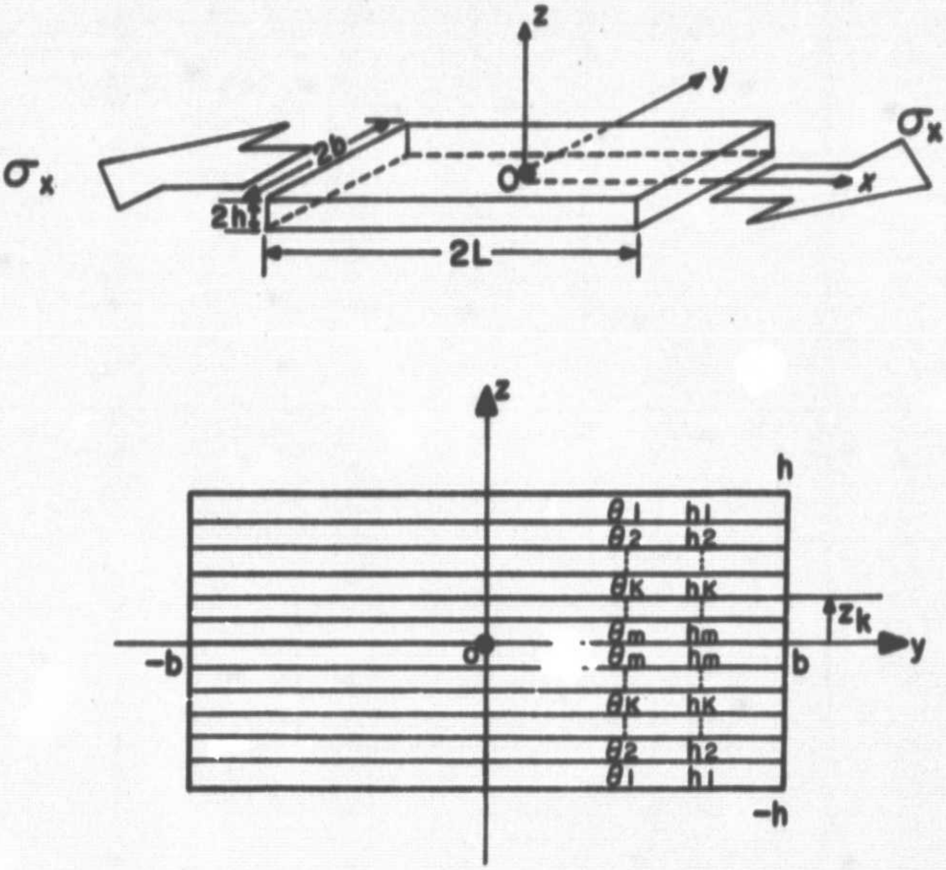

FIGURE 1. LAMINATE GEOMETRY

PRECEDING PAGE BLANK NOT FILMED

NOTE : τ_{xy}, τ_{xz} (NOT SHOWN)

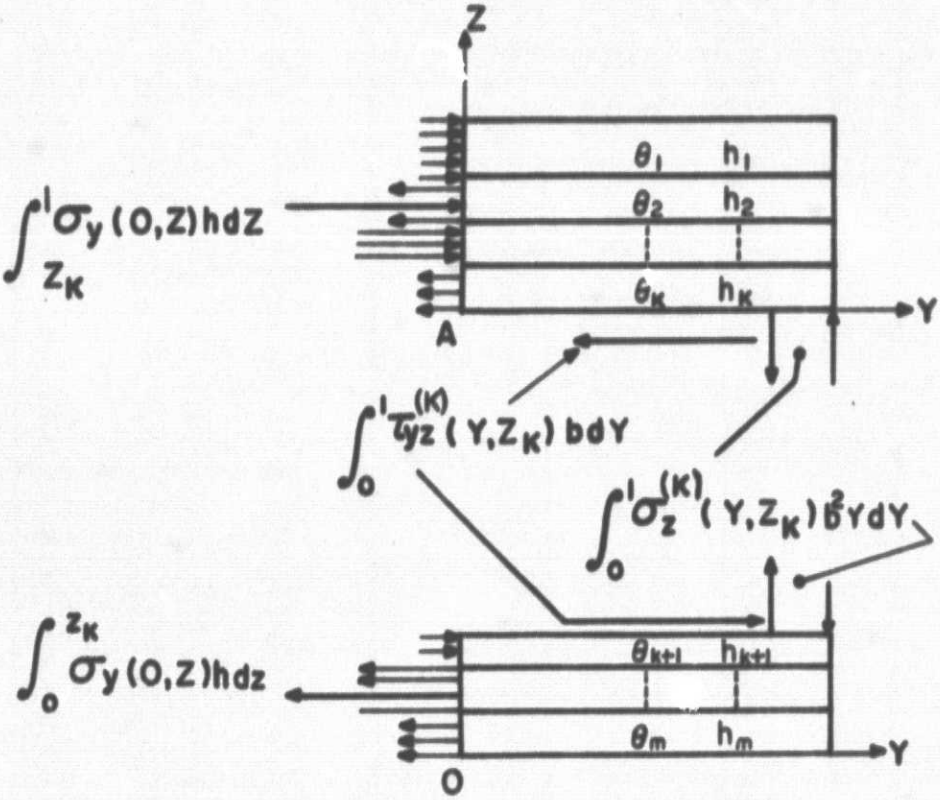

FIGURE 2 FREE BODY DIAGRAM OF QUARTER YZ-PLANE

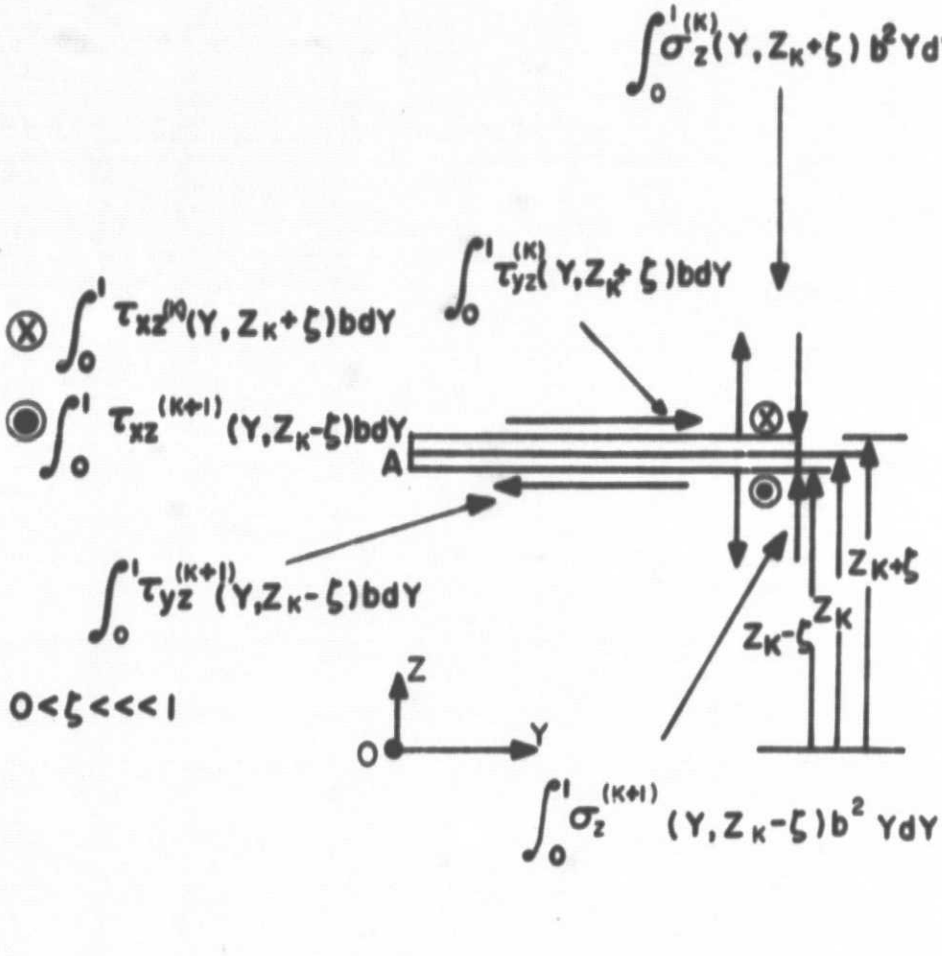

FIGURE 3. LIMITING FREE BODY DIAGRAM OF THE INTERFACE $Z = Z_K$

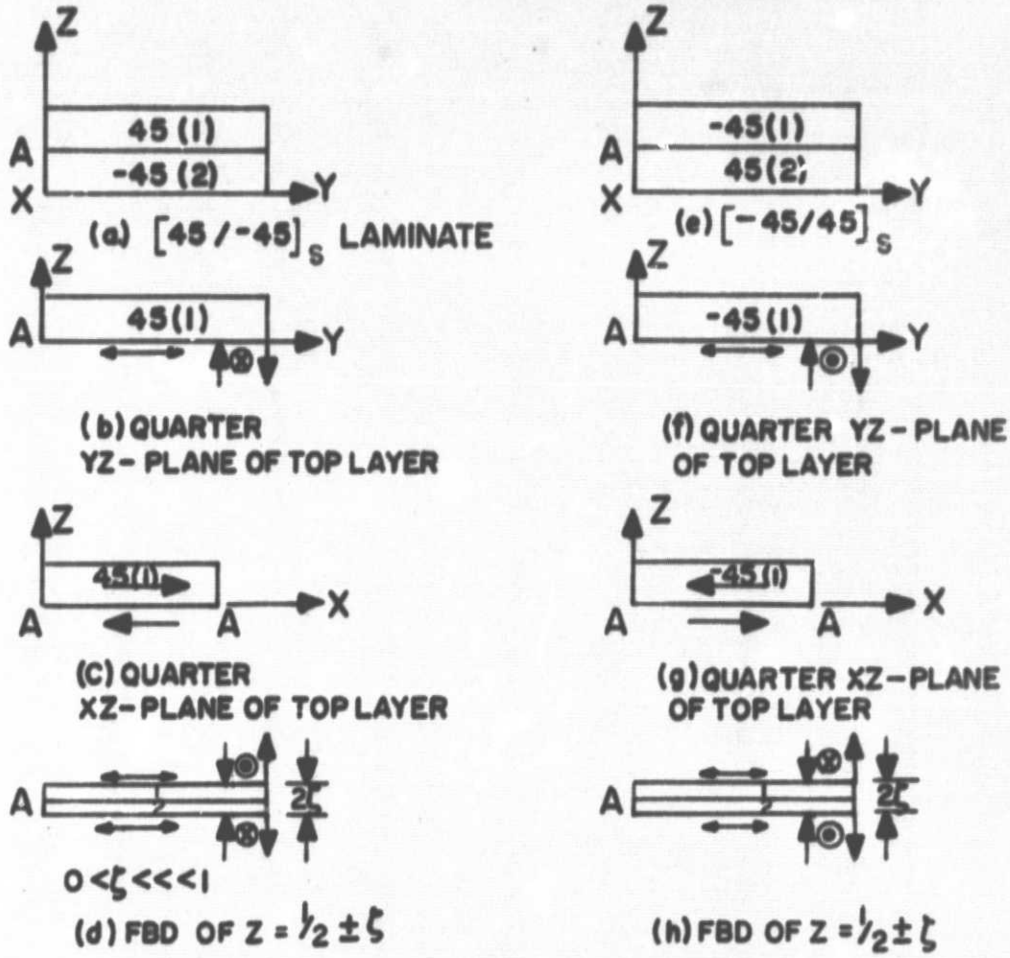

FIGURE 4. FOUR LAYER ANGLE - PLY LAMINATE

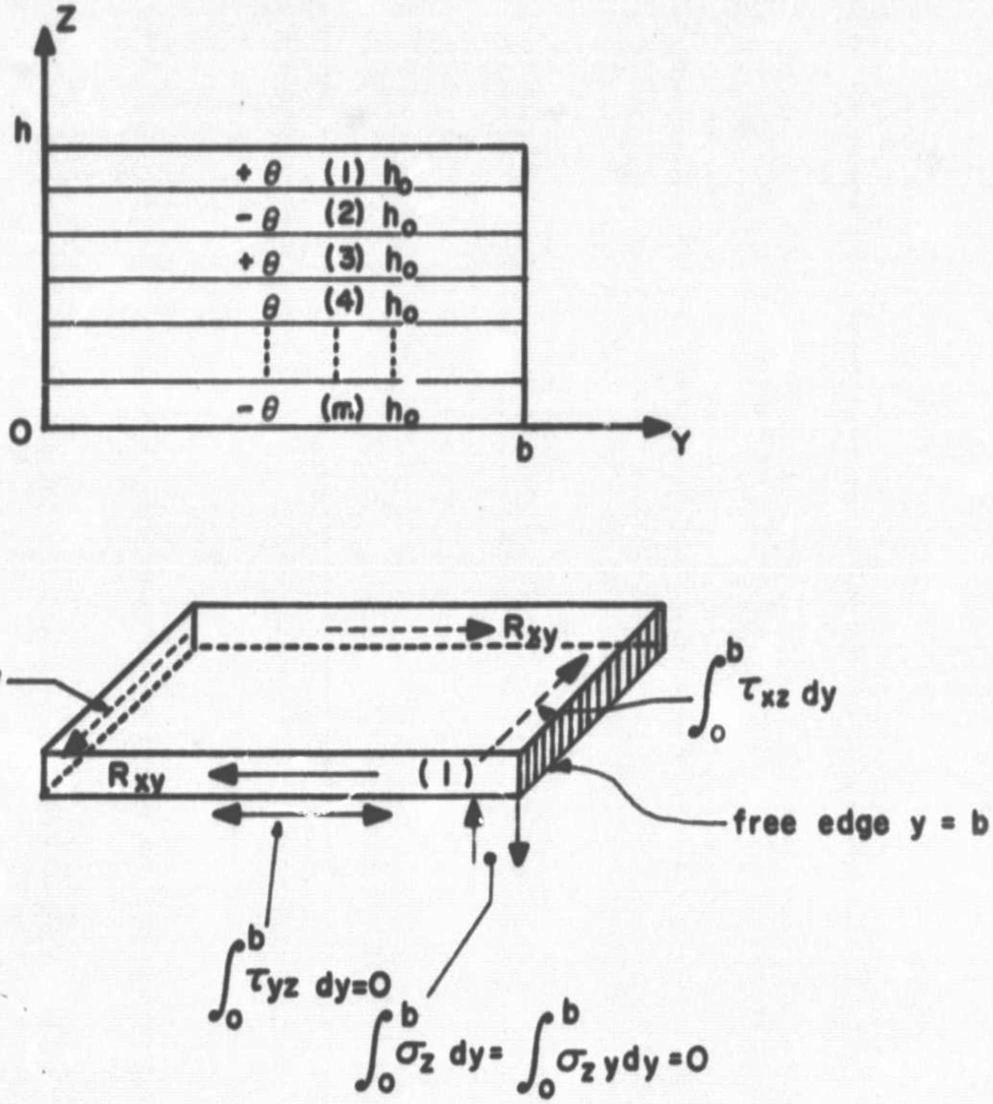

FIGURE 5 ANGLE-PLY LAMINATE OF 2 m LAYERS

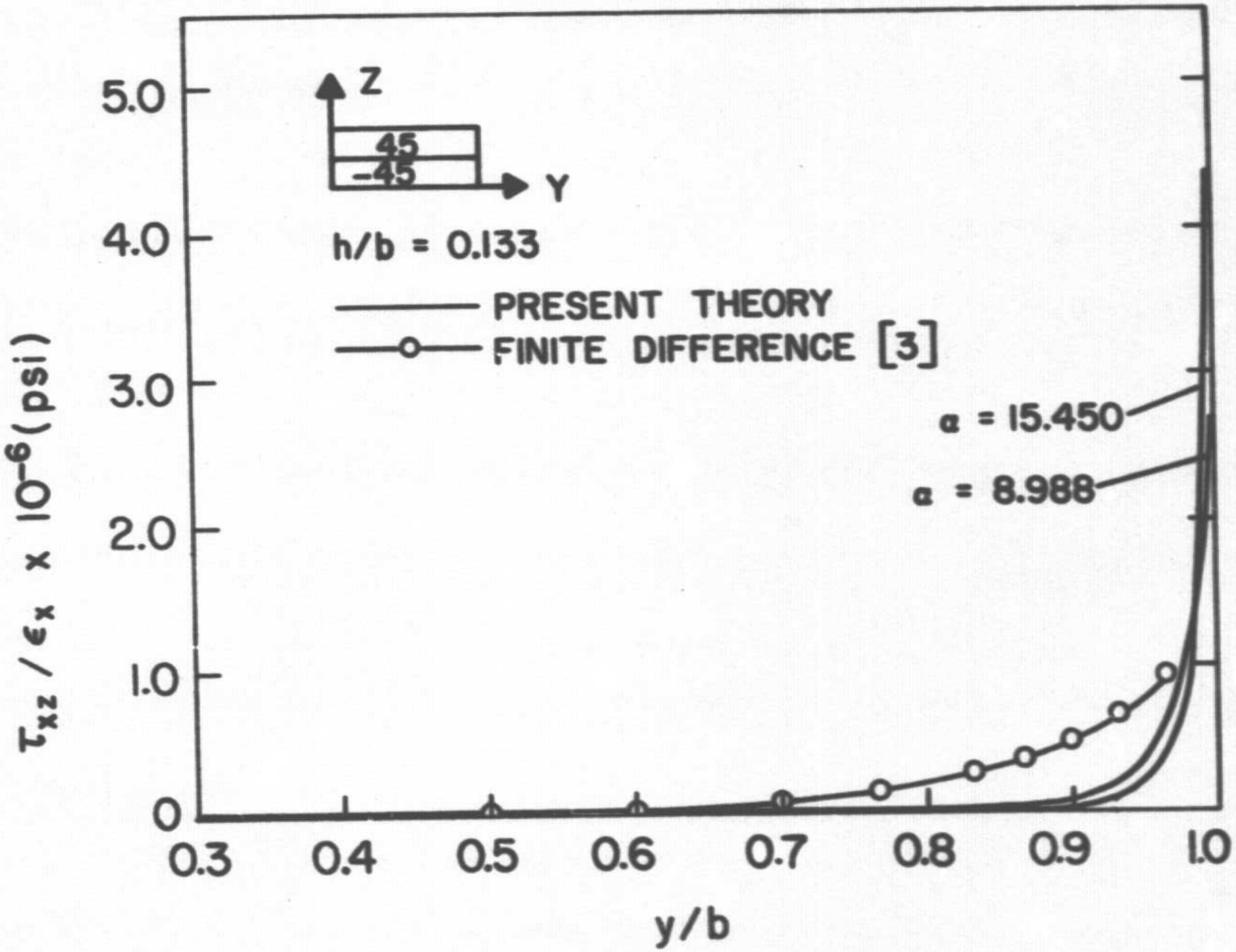

FIGURE 6. PRESENT THEORY AND FINITE DIFFERENCE RESULTS FOR τ_{xz} IN $[45/-45]_s$

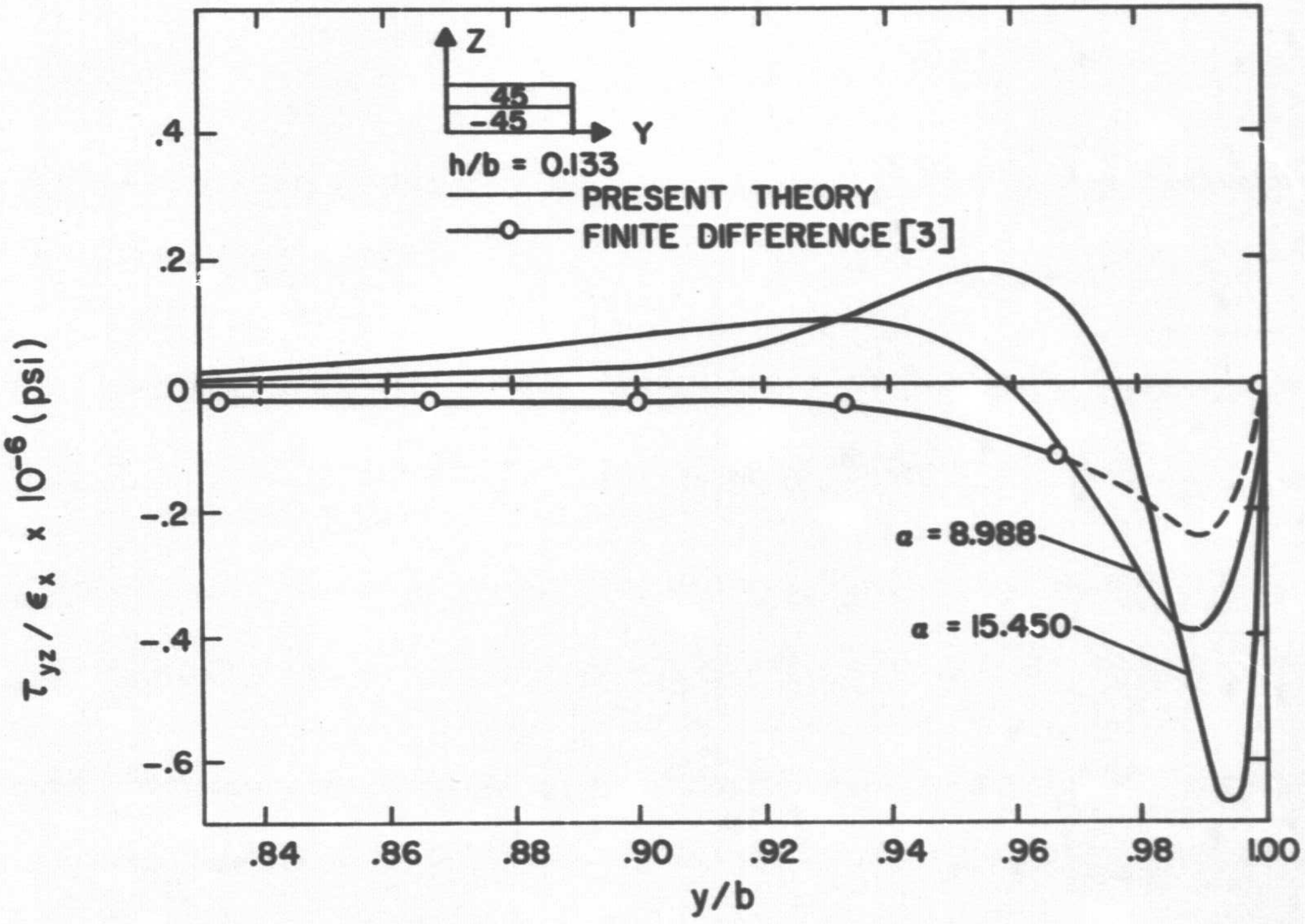

FIGURE 7. PRESENT THEORY AND FINITE DIFFERENCE RESULTS FOR τ_{yz} in $[45/-45]_s$

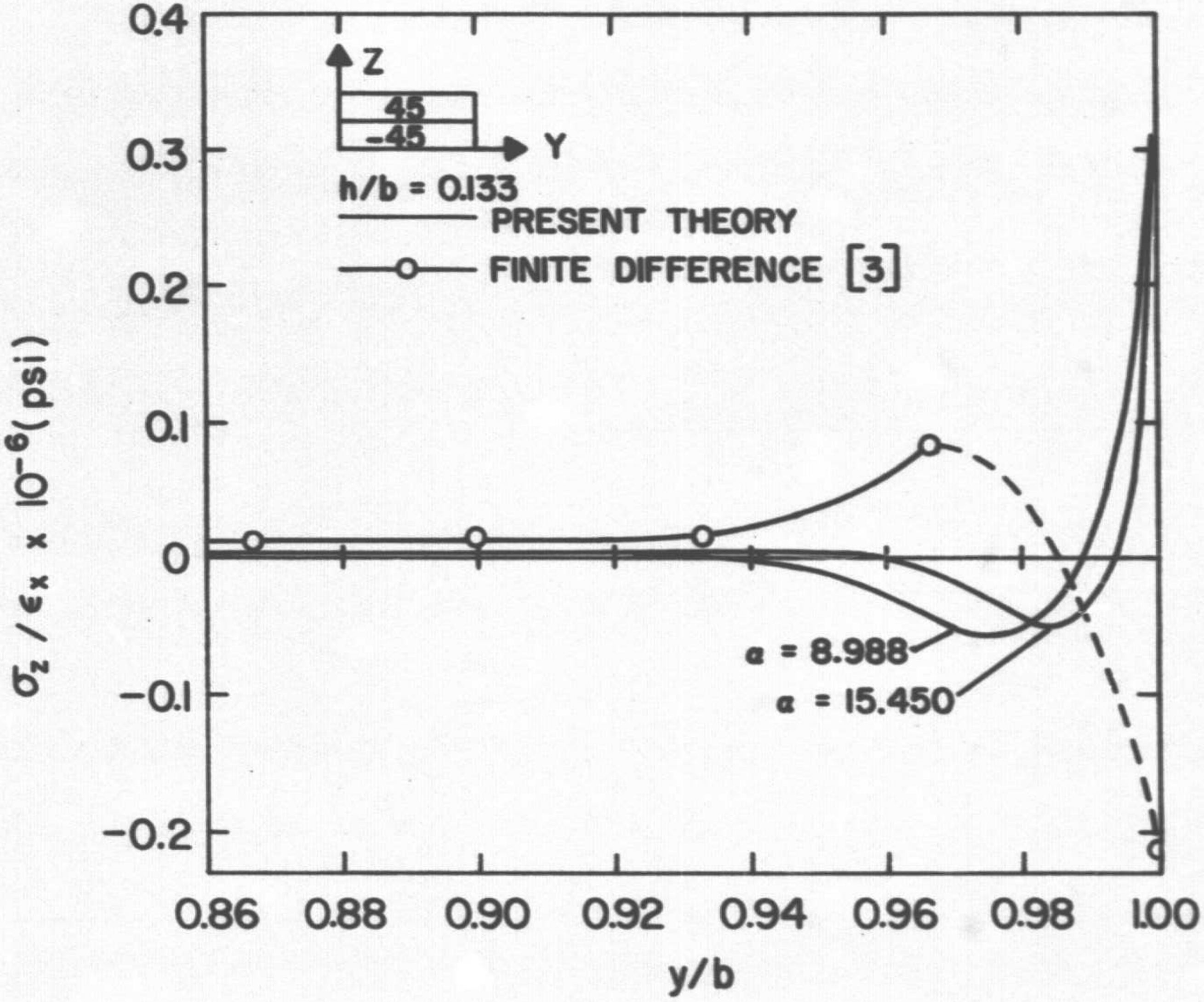

FIGURE 8. PRESENT THEORY AND FINITE DIFFERENCE RESULTS FOR σ_z IN $[45/-45]_s$

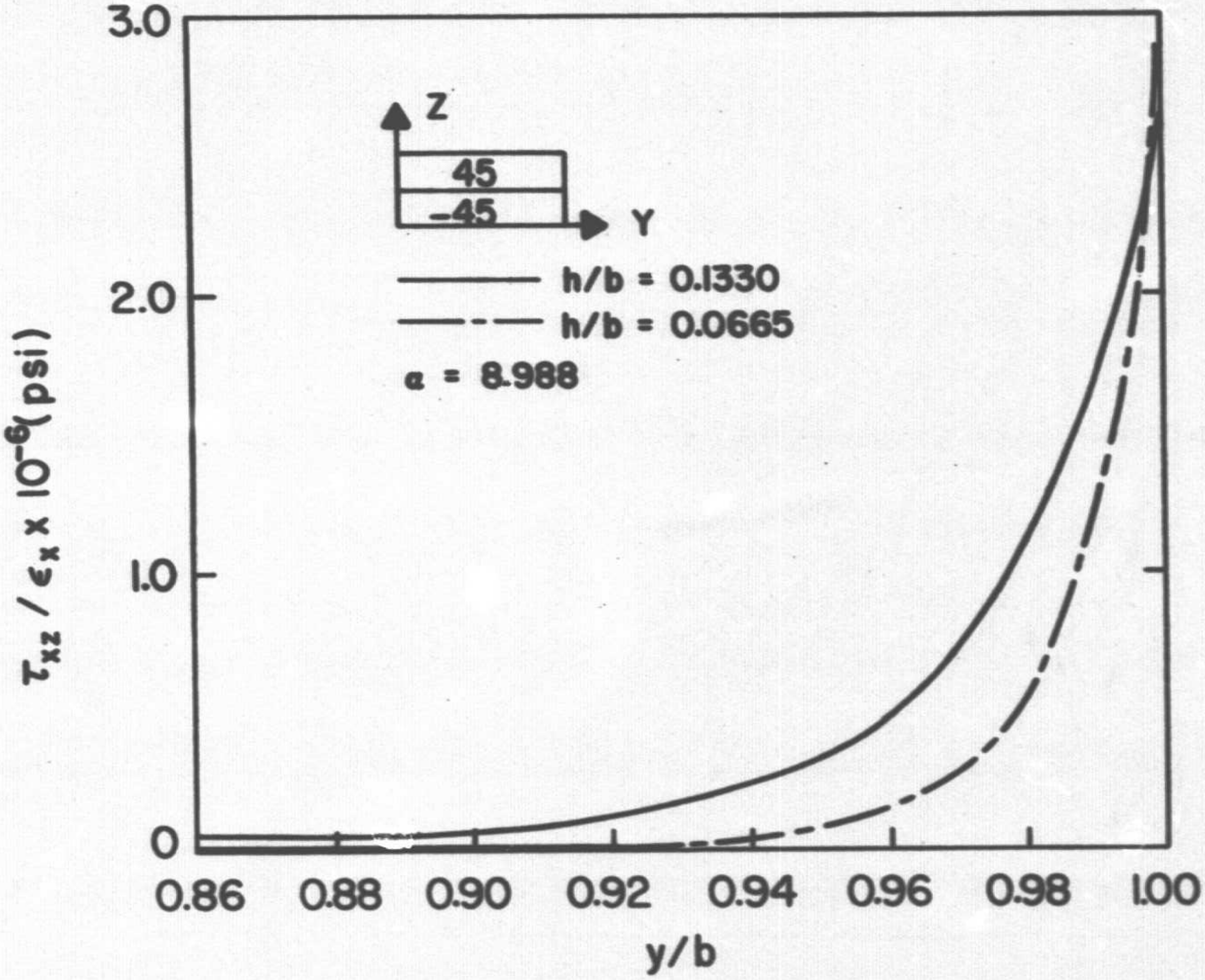

FIGURE 9. INTERLAMINAR SHEAR STRESS τ_{xz} AS A FUNCTION OF h/b IN $[45/-45]_s$

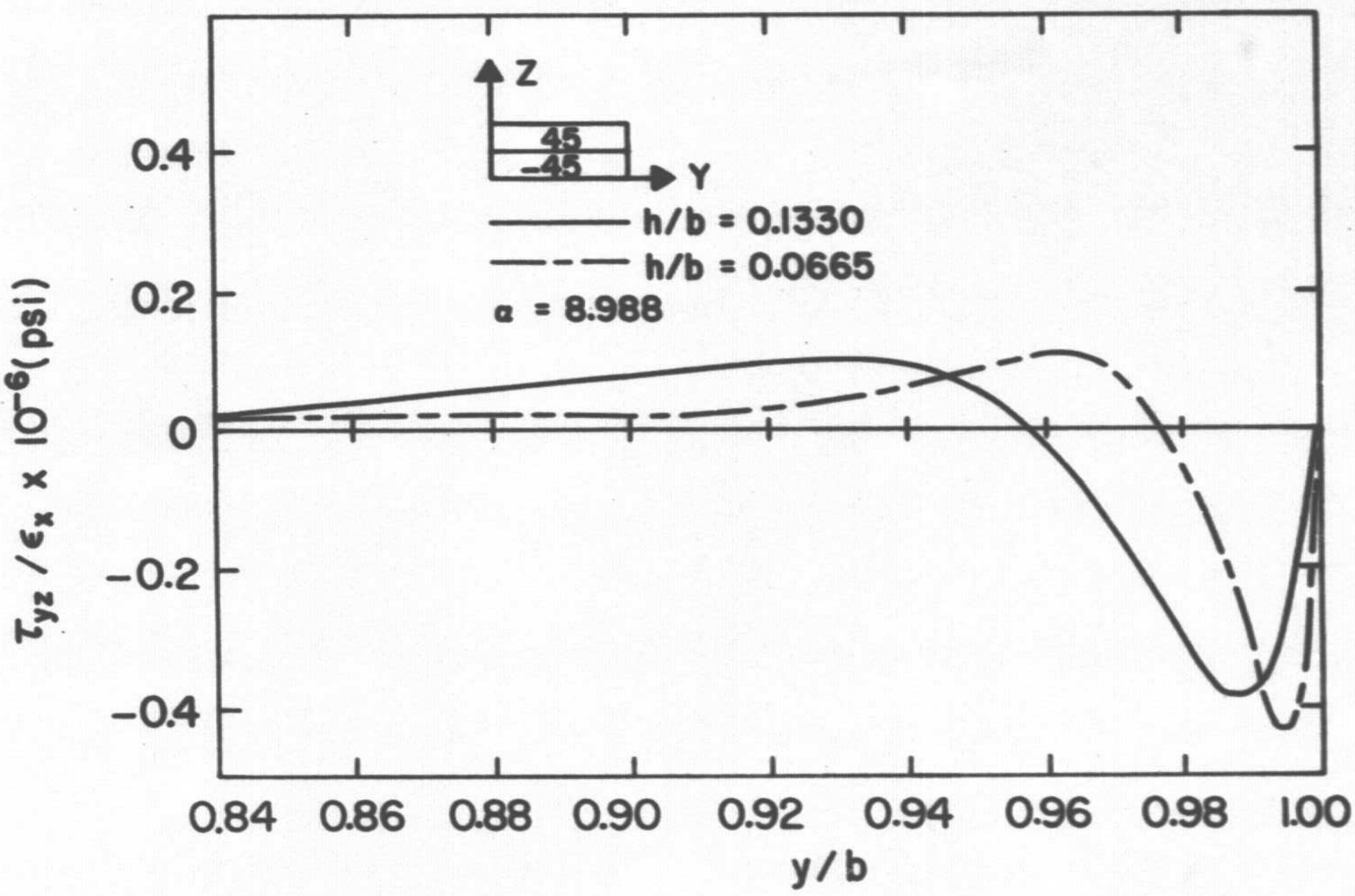

FIGURE 10. INTERLAMINAR SHEAR STRESS τ_{yz} AS A FUNCTION OF h/b IN $[45/-45]_s$

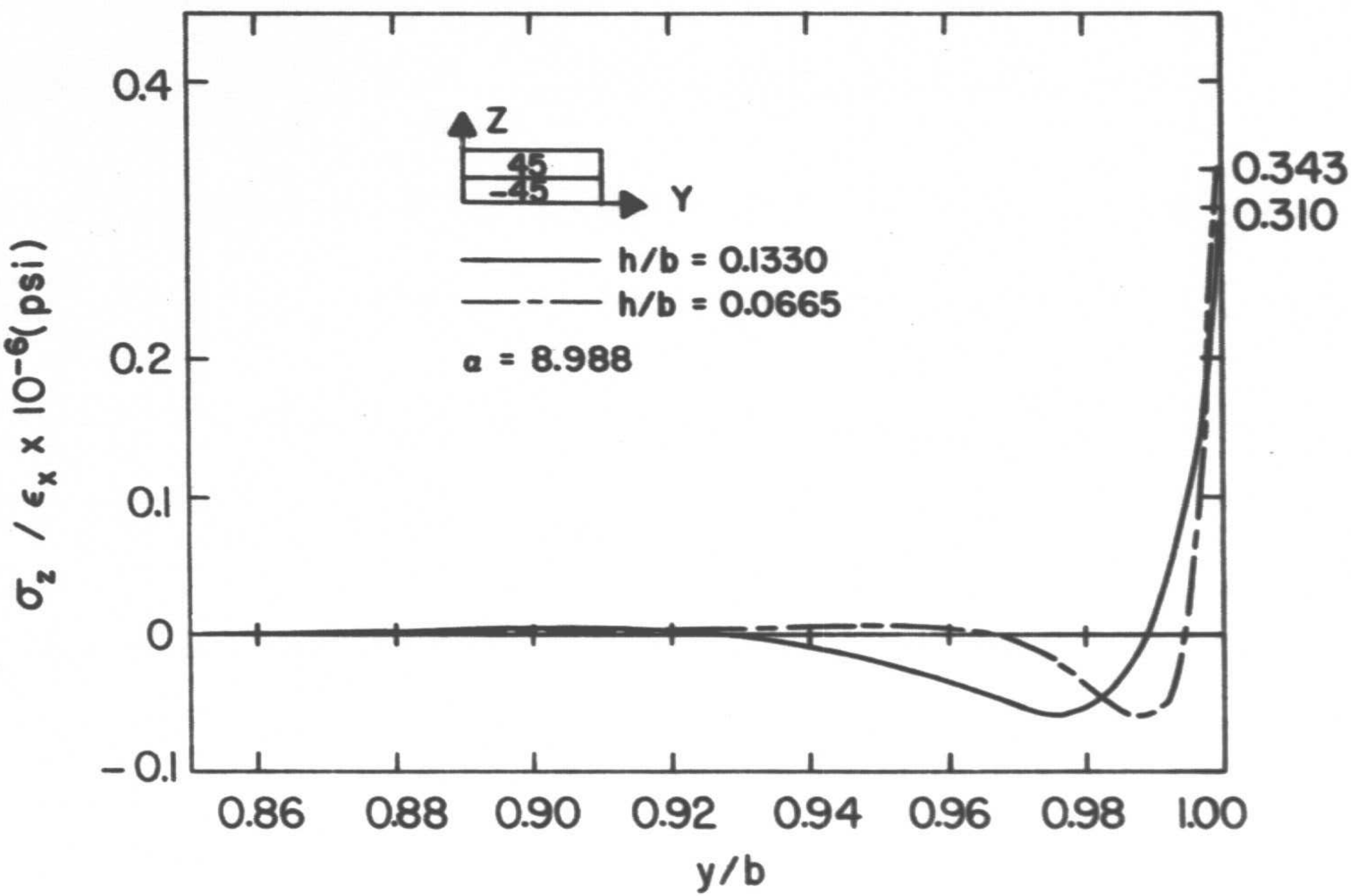

FIGURE 11. INTERLAMINAR NORMAL STRESS σ_z AS A FUNCTION OF h/b IN $[45/-45]_s$